# Stabilization of the Veratryl Alcohol Cation Radical by Lignin Peroxidase†

Aditya Khindaria, Isao Yamazaki,‡ and Steven D. Aust*

*Biotechnology Center, Utah State University, Logan, Utah 84322-4705*

*Received January 23, 1996; Revised Manuscript Received March 18, 1996*⊗

ABSTRACT: Lignin peroxidase (LiP) catalyzes the $H_2O_2$-dependent oxidation of veratryl alcohol (VA) to veratryl aldehyde, with the enzyme-bound veratryl alcohol cation radical ($VA^{\bullet+}$) as an intermediate [Khindaria et al. (1995) *Biochemistry 34*, 16860−16869]. The decay constant we observed for the enzyme-generated cation radical did not agree with the decay constant in the literature [Candeias and Harvey (1995) *J. Biol. Chem. 270*, 16745−16748] for the chemically generated radical. Moreover, we have found that the chemically generated $VA^{\bullet+}$ formed by oxidation of VA by Ce(IV) decayed rapidly with a first-order mechanism in air- or oxygen-saturated solutions, with a decay constant of $1.2 \times 10^3$ $s^{-1}$, and with a second-order mechanism in argon-saturated solution. The first-order decay constant was pH-independent suggesting that the rate-limiting step in the decay was deprotonation. When $VA^{\bullet+}$ was generated by oxidation with LiP the decay also occurred with a first-order mechanism but was much slower, 1.85 $s^{-1}$, and was the same in both oxygen- and argon-saturated reaction mixtures. However, when the enzymatic reaction mixture was acid-quenched the decay constant of $VA^{\bullet+}$ was close to the one obtained in the Ce(IV) oxidation system, $9.7 \times 10^2$ $s^{-1}$. This strongly suggested that the LiP-bound $VA^{\bullet+}$ was stabilized and decayed more slowly than free $VA^{\bullet+}$. We propose that the stabilization of $VA^{\bullet+}$ may be due to the acidic microenvironment in the enzyme active site, which prevents deprotonation of the radical and subsequent reaction with oxygen. We have also obtained reversible redox potential of $VA^{\bullet+}$/VA couple using cyclic voltammetery. Due to the instability of $VA^{\bullet+}$ in aqueous solution the reversible redox potential was measured in acetone, and was 1.36 V vs normal hydrogen electrode. Our data allow us to propose that enzymatically generated $VA^{\bullet+}$ can act as a redox mediator but not as a diffusible oxidant for LiP-catalyzed lignin or pollutant degradation.

Lignin peroxidases (LiP)[1] are largely responsible for lignin and pollutant degradation by the white rot fungus *Phanerochaete chrysosporium* (Barr & Aust, 1994; Kirk & Farell, 1987; Buswell & Odier, 1987; Hammel et al., 1994). These peroxidases are secreted extracellularly at the onset of secondary metabolism and can be induced by nutrient starvation (Tien & Kirk, 1983). Other components of the lignin degrading system, which are also secreted extracellularly at the onset of secondary metabolism, are manganese-dependent peroxidases, oxalate, veratryl alcohol (VA) and $H_2O_2$ generating enzymes (Faison & Kirk, 1985; Kuan & Tien, 1993; Lundquist & Kirk, 1978).

Pertinent to the present study is LiP and its substrate VA. Ferric LiP is oxidized by $H_2O_2$ to an intermediate called compound I. Compound I oxidizes VA to the veratryl alcohol cation radical ($VA^{\bullet+}$) (Khindaria et al., 1995a) and is itself reduced to compound II. Veratryl alcohol cation radical has been shown to form a catalytic complex with compound II (Khindaria et al., 1995b) This compound II−$VA^{\bullet+}$ complex reacts with an additional molecule of VA, resulting in the formation of veratryl aldehyde (VAD). Alternately, in the absence of excess VA the catalytic complex may decay with the release of $VA^{\bullet+}$. Free compound II results, which can react with an additional molecule of VA as in the conventional peroxidase catalytic cycle (Chance, 1952; Tien, 1987; Dunford, 1990).

Direct electron spin resonance (ESR) evidence for the LiP-catalyzed formation of $VA^{\bullet+}$ has recently been reported (Khindaria et al., 1995a). Subsequently it has been shown that the $VA^{\bullet+}$ may not be free in solution but exists as an enzyme-bound species (Khindaria et al., 1995b). It has also been demonstrated that $VA^{\bullet+}$, formed by oxidation with LiP, can act as a redox mediator for indirect oxidations catalyzed by LiP (Chung & Aust, 1995; Goodwin et al., 1995; Koduri & Tien, 1995). However, a recent report by Rao and Tien (1995) demonstrated indirect oxidation of guaiacol by $VA^{\bullet+}$ but questioned whether this would be its physiological role. They argued that $VA^{\bullet+}$ may not be stable and diffusible. This was explored by Candeias and Harvey (1995), who studied the mechanism of decay and the decay constant for $VA^{\bullet+}$, generated by pulse radiolysis. They reported a first-order decay constant of 17 $s^{-1}$ and speculated that it could diffuse a considerable distance. In contrast, we have found that the decay constant of chemically generated $VA^{\bullet+}$ is greater than that reported by Candeias and Harvey (1995) and that it may not be stable enough to act as a diffusible oxidant. However, we have discovered that the decay constant of LiP-bound $VA^{\bullet+}$ is much lower than that for free $VA^{\bullet+}$. On the basis of the observations reported in this study

† This research was supported in part by NIEHS Grant ES04922. A.K. is generously supported by the Utah State University Presidential Fellowship.

* To whom correspondence should be addressed.

‡ Present address: 3-6, North 27, West 11, Sapporo 001, Japan.

⊗ Abstract published in *Advance ACS Abstracts,* May 1, 1996.

[1] Abbreviations: LiP, lignin peroxidase; VA, veratryl alcohol; $VA^{\bullet+}$, veratryl alcohol cation radical; $k_d$, decay constant of veratryl alcohol cation radical formed by oxidation with Ce(IV); $k_{de}$, decay constant of veratryl alcohol cation radical formed by oxidation with lignin peroxidase; NHE, normal hydrogen electrode..

S0006-2960(96)00166-3 CCC: $12.00 

and our earlier results, demonstrating the reaction of LiP-bound $VA^{\bullet+}$ with oxalate (Khindaria et al., 1995b), we propose that it can act as a redox mediator but only as an enzyme-bound species.

## MATERIALS AND METHODS

*Materials.* Hydrogen peroxide, Tempol, and tetranitromethane were purchased from Sigma Chemical Co. Veratryl alcohol was obtained from Aldrich Chemical Co. and vacuum-distilled to free it of a trace contaminant (Tien et al., 1986). Sodium succinate, succinic acid, and $HNO_3$ (69%) were purchased from Mallinckrodt. All chemicals were reagent-grade and were used without further purification, unless otherwise stated. All buffers and solutions were prepared using purified water (Barnstead NANOpure II system; specific resistance 18.0 M$\Omega$ cm$^{-1}$). Pure lignin peroxidase isozyme H2 (p$I$ = 4.4), purified as described previously (Tuisel et al., 1990), was used throughout the study.

*ESR Quantitation of VA$^{\bullet+}$.* The $VA^{\bullet+}$ formed by oxidation with Ce(IV) was quantitated as described previously (Khindaria et al., 1995a). The $VA^{\bullet+}$ formed by oxidation with LiP was also quantitated by ESR using a two-syringe fast-flow system (Khindaria et al., 1995b). For radical quantitation under acid-quenched conditions a three-syringe flow system was used. The contents of the first two syringes, one containing LiP and VA and the other containing $H_2O_2$, were first mixed together for 0.5 s, following which 10% $HNO_3$ was added using the third syringe to acid-quench the reaction and denature the enzyme.

Radical concentrations in both systems were determined by double integration of the first derivative spectra using Tempol as a standard. Standard solution of Tempol was prepared using an extinction coefficient of 1440 M$^{-1}$ cm$^{-1}$ at 240 nm (Morrisett, 1976).

The ESR spectrum obtained by oxidation of VA with Ce(IV) at pH 0 is shown in Figure 1A. The hyperfine splitting constants of the radical signal are identical to those published previously for $VA^{\bullet+}$ (Khindaria et al., 1995a). The concentration of the radical (Figure 1A) was calculated to be 15.8 $\mu$M by double integration of the ESR spectrum and using Tempol as a standard. A similar spectrum obtained in oxygen-saturated solution is shown as Figure 1B. The ESR spectra of the $VA^{\bullet+}$ obtained in the LiP oxidation system under normal turnover and under acid-quenched conditions are shown in Figure 1, panels C and D, respectively.

*Rate Constant for Reaction of Ce(IV) and VA.* Stock Ce(IV) solutions were prepared in water. Appropriate aliquots of this were diluted to a final concentration of 3 mM. This was then mixed with at least 10 mM VA (to ensure pseudo-first-order kinetics). The reduction of Ce(IV) to Ce(III) was followed as a decrease in absorbance at 380 nm in a stopped-flow spectrophotometer (KinTek Instruments, State College, PA). The stopped-flow acquisition was fit to a first-exponential equation to obtain the rate of Ce(IV) reaction with VA, $k_{obs}$.

*Computer simulations* of the experimental data were performed with the kinetic simulation program KINSIM (Barshop et al., 1983), provided by Carl Frieden and Bruce Barshop (Washington University, St. Louis, MO).

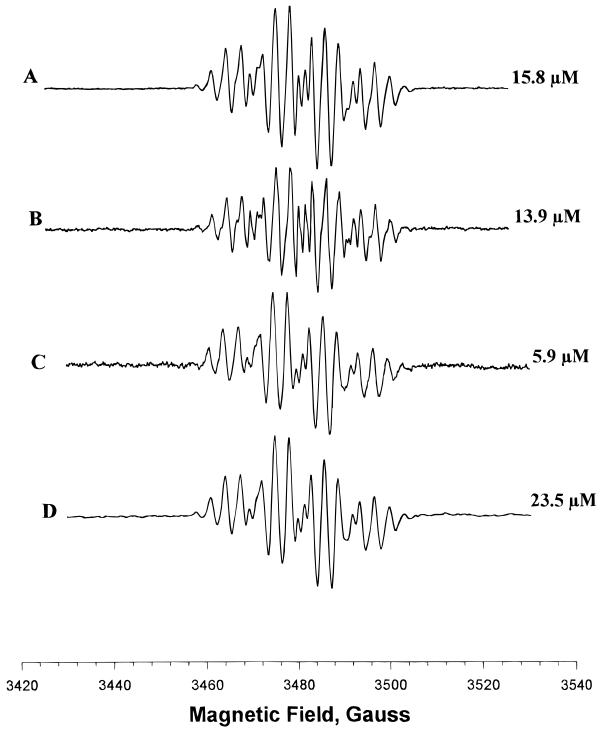


FIGURE 1: ESR spectra of $VA^{\bullet+}$. Spectrum A was recorded in an argon-saturated reaction mixture containing 1 mM Ce(IV) and 10 mM VA at pH 0. Spectrum B was recorded under the same conditions as A except that the reaction mixture was saturated with oxygen. Spectrum C was recorded in a reaction mixture containing 25 $\mu$M LiP, 2 mM VA, and 200 $\mu$M $H_2O_2$ in pH 4.5 succinate buffer. Spectrum D was recorded under the same reaction conditions as C except that 10% $HNO_3$ was added to the reaction cell immediately before the acquisition. The numbers on the right are the concentrations of the radical as determined by double integration of the spectrum and using Tempol as a standard.

## RESULTS AND DISCUSSION

*Oxidation of VA by Ce(IV).* Cerium(IV) was able to oxidize VA as determined by the decrease in absorbance at 380 nm due to the reduction of Ce(IV) to Ce(III). The rate of Ce(IV) reduction was dependent on VA concentration. A stopped-flow trace for 1 mM Ce(IV) and 10 mM VA is shown in the inset to Figure 2. The $k_{obs}$ values, obtained by fitting traces to a first-exponential equation, were plotted against the concentration of VA (Figure 2). The slope of the plot gives the second-order rate constant for the reaction of Ce(IV) with VA to be $3 \times 10^3$ M$^{-1}$ s$^{-1}$ at pH 1.2. The rate constant for the reaction of Ce(IV) and VA decreased with increasing pH (data not shown).

The product of VA oxidation by Ce(IV) was $VA^{\bullet+}$, as confirmed by the ESR signal obtained using a two-syringe continuous-flow system described previously (Khindaria et al., 1995). The spectra were recorded during continuous flow at a high modulation amplitude at the optimum (for maximum ESR signal) flow rate. The steady-state concentration of $VA^{\bullet+}$ as a function of VA concentration at fixed concentration of Ce(IV) (2.5 mM) is shown in Figure 3, plot a. The plot was linear and the data were used to calculate the decay constant ($k_d$) by using

$$\frac{d[VA^{\bullet+}]}{dt} = k[\text{Ce(IV)}][\text{VA}] - k_d[VA^{\bullet+}] \qquad (1)$$

where $k$ is the rate constant for the reaction of VA with Ce-

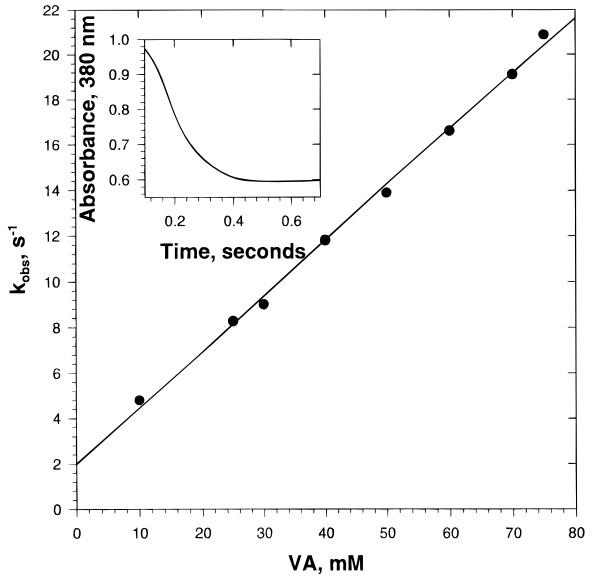


FIGURE 2: Rates of reduction of Ce(IV) by VA as a function of VA concentration. The reduction of Ce(IV) was followed at 380 nm under pseudo-first-order conditions with the concentration of VA being at least 10 times the concentration of Ce(IV) in the reaction mixture. The $k_{obs}$ values were determined by fitting the stopped-flow traces (inset; $k_{obs} = 4.7$ with 10 mM VA) to a first exponential equation. The second-order rate constant for the reaction of Ce(IV) with VA, as determined from the slope of the plot was $3.0 \times 10^3$ $M^{-1}$ $s^{-1}$. Each datum point is an average of at least three acquisitions.

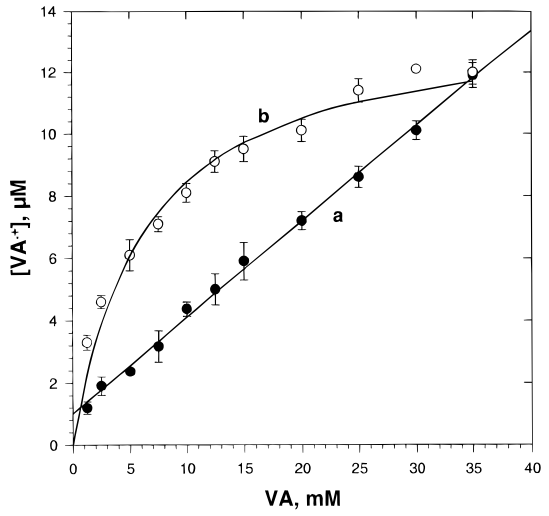


FIGURE 3: Effect of VA concentration on the steady-state concentration of $VA^{\bullet+}$ formed by oxidation of VA by a constant concentration of 2.5 mM Ce(IV) . All ESR spectra were recorded at pH 1.2 under oxygen/air- (●) or argon- (○) saturated conditions during continuous flow (24 mL/min) and the concentrations of the radical were determined by double-integrating the ESR spectra and using Tempol as a standard. The data points are an average of three acquisitions and the error bars represent standard deviations.

(IV) and $k_d$ is the decay constant of $VA^{\bullet+}$. At steady-state $d[VA^{\bullet+}]/dt = 0$. Therefore eq 1 can be rearranged as follows:

$$k_d[VA^{\bullet+}] = k[Ce(IV)][VA]$$

or

$$[VA^{\bullet+}] = (k[Ce(IV)][VA])/k_d$$

Thus the slope of plot a is equal to $k[Ce(IV)]/k_d$. From the slope, the decay constant, $k_d$, for $VA^{\bullet+}$ was calculated to be $1.2 \times 10^3$ $s^{-1}$. The decay constant, $k_d$, was found to be pH-independent (data not shown). The first order, pH independent decay constant suggested that the decay of the radical was due to deprotonation in the following equilibrium reaction.

$$VA^{\bullet+} \underset{k_{-1}}{\overset{k_1}{\rightleftharpoons}} VA^{\bullet} + H^+ \quad (2)$$

In the presence of oxygen, protonation would be negligible because of the rapid reaction of $O_2$ with $VA^{\bullet}$

$$VA^{\bullet} + O_2 \rightarrow VAOO^{\bullet} \quad (3)$$

which occurs at near diffusion-limited rates and subsequently VAD is formed according to

$$VAOO^{\bullet} \rightarrow VAD + HO_2 \quad (4)$$

Therefore, the measured decay constant equals the deprotonation rate constant ($k_1$). Our value for deprotonation of $VA^{\bullet+}$ is in contrast with the value of 17 $s^{-1}$ reported by Candeias and Harvey (1995). Though it is difficult to compare the two values because of different methods of determination under different experimental conditions, their value is suspect mainly because the literature data for deprotonation of similar cation radicals (Schmidt et al., 1985; Hammerich & Parker, 1984) support the value obtained in this study.

To further investigate the role of oxygen in the decay of $VA^{\bullet+}$, we carried out the same reaction in argon-saturated solution. The plot of the steady-state concentration of $VA^{\bullet+}$ versus the concentration of VA best fit a second-order equation (Figure 3, plot b). From the initial slope of the plot it was evident that the decay of $VA^{\bullet+}$ was slower in argon-saturated than in oxygen-saturated solutions. The deviation of plot b from linearity was explained by considering the dismutation reaction (eq 5) and the reaction of $VA^{\bullet+}$ with $VA^{\bullet}$ (eq 6):

$$2VA^{\bullet} \xrightarrow{k_2} VA + VAD \quad (5)$$

$$VA^{\bullet+} + VA^{\bullet} \xrightarrow{k_3} VA + VAD + H^+ \quad (6)$$

The final equation defining plot b is a complex function of $k_1$ and $k_{-1}$, the protonation and deprotonation rate constants, respectively, $k_2$, the dismutation rate constant for $VA^{\bullet}$, $k_3$, the rate constant for the reaction of $VA^{\bullet+}$ with $VA^{\bullet}$, and the concentrations of the species involved. Though it is possible to numerically solve the equation to obtain its roots, a relevant nontrivial solution for the function cannot be obtained at this stage. To obtain a nontrivial solution to the equation, several parameters including rate constants for various reactions of $VA^{\bullet}$ will have to be obtained empirically. Our attempts to detect (direct ESR) or spin-trap $VA^{\bullet}$ were not successful. Under aerobic conditions this was probably due to the rapid reaction of $VA^{\bullet}$ with $O_2$ and under anaerobic conditions due to the reaction of $VA^{\bullet}$ with $VA^{\bullet+}$. The rates of both these reactions are predicted to be greater than $10^8$ $M^{-1}$ $s^{-1}$. However, it is important to note that a second-order reaction is rate-limiting in the decay of $VA^{\bullet+}$ under

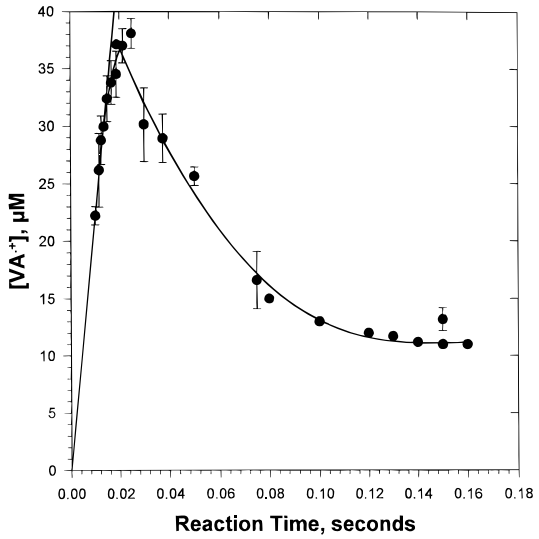


FIGURE 4: Effect of reaction time on the concentration of $VA^{\bullet+}$, formed by oxidation of VA by Ce(IV). The reaction mixture contained 2.5 mM Ce(IV) and 25 mM VA at pH 1.2. The ESR spectra were recorded during continuous flow and the concentrations of $VA^{\bullet+}$ were determined as described in the Materials and Methods section. The reaction time was adjusted by varying the flow rate through the capillary cell (1 $\mu$L). The reaction time was calculated by dividing half the cell volume by the flow rate. The line is the kinetic simulation of the experimental data using eqs 1 and 2, with $k = 2.4 \times 10^3$ $M^{-1}$ $s^{-1}$ and $k_d = 1.1 \times 10^3$ $s^{-1}$. The initial linear increase is equal to the rate constant for the reaction of VA with Ce(IV). The data points are an average of three acquisitions and the error bars represent standard deviations.

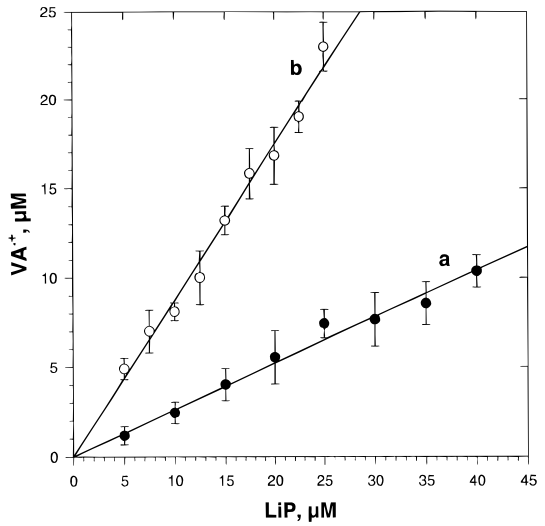


FIGURE 5: Effect of varying the concentration of LiP on the steady-state concentration of $VA^{\bullet+}$ under normal turnover and acid-quenched conditions. During normal turnover (plot a; ●) the reaction mixture contained 2 mM VA, 200 $\mu$M $H_2O_2$, and the indicated concentration of LiP in pH 4.5 succinate buffer. Under acid-quenched conditions (plot b; ○), a three-syringe system was used for acquiring the ESR spectra to determine the concentration of $VA^{\bullet+}$. The contents of the first two syringes, the first containing LiP (indicated concentration), and the second containing VA (2 mM) and $H_2O_2$ (200 $\mu$M), were first mixed in the delay line for 0.5 s, following which 10% $HNO_3$ was mixed from a third syringe. The data points are an average of three acquisitions and the error bars represent standard deviations.

argon-saturated conditions. Probably $VA^{\bullet+}$ is in equilibrium with $VA^{\bullet}$ as in reaction 2 but decays through reactions 5 and 6.

Additional kinetic analysis was performed by determining the concentration of $VA^{\bullet+}$ as a function of reaction time. At a constant concentration of both Ce(IV) and VA, the flow rate through the ESR capillary cell (1 $\mu$L dead volume) was varied. The concentration of $VA^{\bullet+}$ was measured during continuous flow and is shown as a function of reaction time (or mean residence time) in the ESR capillary cell (Figure 4, closed circles). The reaction time was calculated by dividing half the dead volume by the flow rate. The slope pertaining to the initial linear increase is equivalent to the reaction rate constant for Ce(IV) with VA. The line in Figure 4 represents the kinetic simulation of eqs 1 and 2 and using the values of $2.4 \times 10^3$ $M^{-1}$ $s^{-1}$ and $1.1 \times 10^3$ $s^{-1}$ for $k$ and $k_d$, respectively. The simulated data agreed closely with the experimental observations and served to verify the rate constant, $k$, and the decay constant, $k_d$, obtained earlier (Figures 2 and 3), even though there are slight discrepancies from the values obtained from the experiments shown in Figures 2 and 3.

*ESR Analysis of $VA^{\bullet+}$ Formed by Oxidation with LiP.* The steady-state concentration of $VA^{\bullet+}$, measured during continuous flow, was plotted as a function of LiP concentration (Figure 5, plot a). One syringe contained $H_2O_2$ and VA and the second contained varying concentrations of LiP. Each datum point was recorded at an optimum flow rate to obtain the maximum ESR signal due to $VA^{\bullet+}$ for the particular concentration of LiP. The linear correlation between the concentration of $VA^{\bullet+}$ and the concentration of LiP suggested that $VA^{\bullet+}$ generated by oxidation with LiP decayed by a pseudo-first-order process. However, a simple first-order

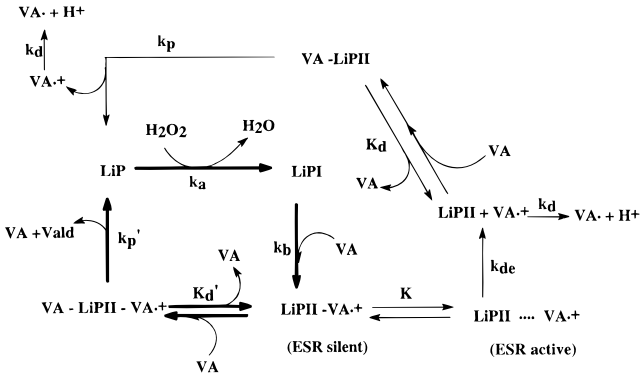


FIGURE 6: Proposed mechanism for the oxidation of VA by LiP. This mechanism was used for simulation of the experimental data in Figure 8. The kinetic constants used for the kinetic simulation were $k_a = 5.6 \times 10^5$ $M^{-1}$ $s^{-1}$, $k_b = 3.3 \times 10^5$ $M^{-1}$ $s^{-1}$, $K'_d = 133$ $\mu$M, $k'_p = 8.3$ $s^{-1}$, $K = 0.14$, $k_{de} = 1.85$ $s^{-1}$, $K_d = 326$ $\mu$M, $k_d = 1.2 \times 10^3$ $s^{-1}$, and $k_p = 5.0$ $s^{-1}$.

equation cannot be used to calculate the decay of $VA^{\bullet+}$ formed by oxidation with LiP. This is because there are two states of $VA^{\bullet+}$ bound to LiPII, one ESR-active and the other ESR-silent (LiPII−$VA^{\bullet+}$; Khindaria et al., 1995b) (Figure 6). Only 13% of the $VA^{\bullet+}$ exists in the ESR-active state as determined from the distribution coefficient between the two states. The mathematical treatment to calculate the decay constant is difficult as 87% of $VA^{\bullet+}$ is involved in the catalytic cycle. The distribution coefficient was further confirmed by determining the concentration of $VA^{\bullet+}$ under acid-quenched conditions. The concentration of $VA^{\bullet+}$ as a function of LiP concentration under these conditions is shown in Figure 5, plot b. The concentration of $VA^{\bullet+}$ detected under these conditions was higher than under normal turnover. The ratio of the slopes (plot a:plot b) was 0.14, in

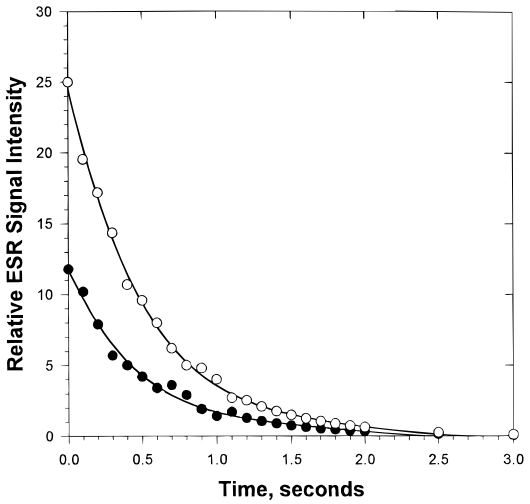


FIGURE 7: Decay of LiPII−$VA^{\bullet+}$ ESR signal. The reaction mixture contained 30 (●) or 40 (○) $\mu$M LiP and equimolar amounts of VA and $H_2O_2$ in a pH 4.5 succinate buffer in a continuous-flow system. Acquisitions were started immediately after the flow was stopped. Static field time sweep was used with the modulation amplitude being 5.0 G.

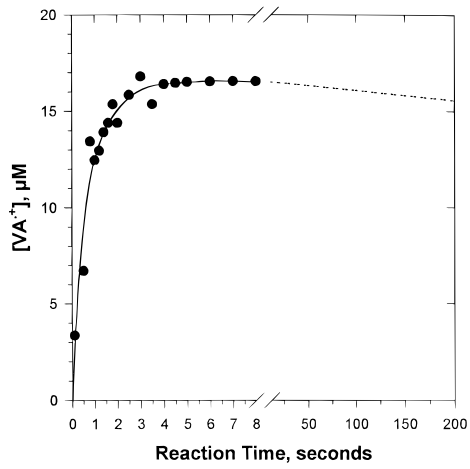


FIGURE 8: Effect of varying reaction time on the concentration of $VA^{\bullet+}$ formed by oxidation with LiP. The reaction mixture contained 40 $\mu$M LiP, 200 $\mu$M $H_2O_2$, and 2 mM VA in pH 4.5 succinate buffer. The ESR data (●) were recorded as explained in the legend to Figure 4. The line is the kinetic simulation of the experimental data using the mechanism given in Figure 6; the kinetic constants used are given in the legend to that figure.

close agreement with the fraction mentioned above (Khindaria et al, 1995b). As explained earlier, the detection of lower concentration of $VA^{\bullet+}$ during turnover was due to the majority of $VA^{\bullet+}$ (87%) existing in the ESR-silent state. This was probably a consequence of spin coupling between the heme iron and $VA^{\bullet+}$. Upon acid quenching the enzyme is denatured and the radical is released into the solution, where it can be detected.

To determine the decay constant of LiP-bound $VA^{\bullet+}$ ($k_{de}$), equimolar amounts of LiP, VA, and $H_2O_2$ were mixed using a stopped-flow ESR system. As is clear from Figure 6, if equimolar VA and $H_2O_2$ are mixed with LiP, then LiPI can be assumed to be reduced quantitatively to LiPII with the concomitant formation of LiPII−$VA^{\bullet+}$. This is because there is dependence on another molecule of VA to complete the catalytic cycle (bold lines). In the absence of excess VA, LiPII−$VA^{\bullet+}$ decays through the dissociation of $VA^{\bullet+}$, which is the rate-limiting step. Therefore, the ESR-active form and ESR-silent form are in equilibrium and can be considered one species. High modulation amplitude and static field time-sweep were employed to observe the decay of LiP-bound $VA^{\bullet+}$ after the flow was stopped. The decrease in the $VA^{\bullet+}$ ESR signal intensity as a function of time is shown in Figure 7 for two different equimolar concentrations of LiP, VA and $H_2O_2$. The decay was first-order in character and the rate constant was 1.85 $s^{-1}$. A similar value was obtained in a reaction mixture saturated with argon. This value is identical to the one reported from the decay of the initial burst of enzyme activity that was measured by the rapid reaction of the LiPII−$VA^{\bullet+}$ complex with VA (Khindaria et al., 1995b).

To further verify the decay constant of the LiP-bound $VA^{\bullet+}$ we repeated the flow-rate-dependent ESR experiments as explained in Figure 4 for the enzymatic reaction system. The concentrations of LiP, VA, and $H_2O_2$ were kept constant and the flow rate through the capillary cell was varied. The concentration of $VA^{\bullet+}$ as a function of reaction time is plotted in Figure 8 (closed circles). The solid line is the computer simulation of the mechanism shown in Figure 6, using the kinetic constants published previously (Khindaria et al., 1995b) and the decay constants for free and LiP-bound $VA^{\bullet+}$ determined in this study. The dashed line is the predicted concentration of $VA^{\bullet+}$ at the indicated reaction time. However, data could not be collected for these time points as the concentration of $H_2O_2$ required would inactivate the enzyme. The computer simulation agreed closely with the experimental data and served to verify the kinetic constants obtained experimentally.

The decay constant for LiP-bound $VA^{\bullet+}$ is about 700 times smaller than the decay constant for free $VA^{\bullet+}$. This suggested that LiP was stabilizing $VA^{\bullet+}$ which would otherwise decay rapidly in bulk solution. To test this hypothesis we investigated the decay of $VA^{\bullet+}$ also formed by oxidation with LiP but under acid-quenched conditions. If indeed LiP was stabilizing $VA^{\bullet+}$, then the denatured enzyme would be incapable of doing so and $VA^{\bullet+}$ should decay at a rate similar to the one obtained in the Ce(IV) oxidation system. In this case the decrease in ESR signal of the $VA^{\bullet+}$ (as in Figure 7) could not be followed due to the extremely rapid decay of free $VA^{\bullet+}$. Therefore, the acid-quenched reaction mixture was flowed through the ESR cell at varying flow rates and the concentration of $VA^{\bullet+}$ at the resultant reaction time was determined from the ESR spectrum. As shown in Figure 9, the concentration of the $VA^{\bullet+}$ decreased rapidly with the increase in reaction time (residence time). The decrease in the concentration of $VA^{\bullet+}$ was best fit to a first-order decay equation with the decay constant of $9.7 \times 10^2$ $s^{-1}$. As predicted, this value is in close agreement with the decay constant obtained in the Ce-(IV) oxidation system.

*Effect of Oxygen on the Steady-State Concentration of* $VA^{\bullet+}$. We then asked whether oxygen would affect the concentration of LiP-bound $VA^{\bullet+}$ as it does free $VA^{\bullet+}$ (Figure 3). The rationale for this experiment was that the deprotonation product of $VA^{\bullet+}$, the neutral radical, reacts at diffusion limited rates with oxygen according to eq 3. Hence, if $VA^{\bullet+}$ is stabilized in the LiP active site, due to a decrease in the rate of deprotonation, the effect of oxygen on equilibrium 2 would be minimal and the concentration of $VA^{\bullet+}$ would not be affected. The effect of oxygen on the

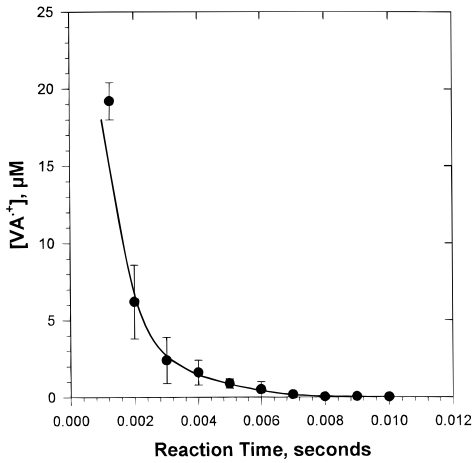


FIGURE 9: Decay of $VA^{\bullet+}$ formed by oxidation with LiP under acid-quenched conditions. A three-syringe flow system was used. The contents of the first two syringes (20 $\mu$M LiP, 2 mM VA, and 200 $\mu$M $H_2O_2$) were first mixed in a delay line for 0.5 s, following which 10% $HNO_3$ was added with the third syringe. The resultant reaction mixture was flowed through the ESR cell at different flow rates to obtain the relevant residence times. The steady-state concentration for the $VA^{\bullet+}$ was calculated from the ESR spectra obtained during continuous flow. The data points are an average of three acquisitions and the error bars represent standard deviations.

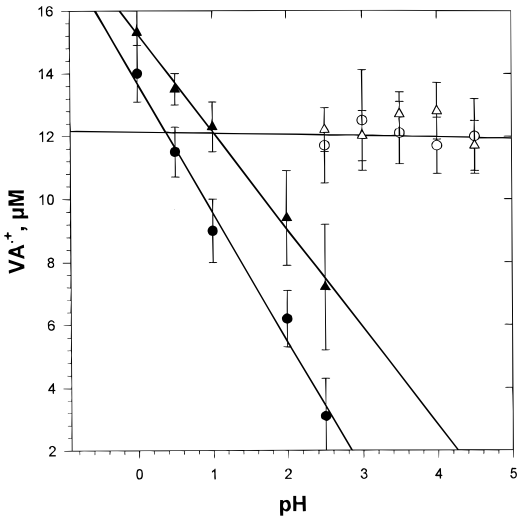


FIGURE 10: Effect of oxygen on the concentration of $VA^{\bullet+}$ formed by oxidation with Ce(IV) and LiP as a function of pH. The closed circles represent the concentration of $VA^{\bullet+}$ when 1 mM Ce(IV) was mixed with 10 mM VA in an oxygen-saturated reaction mixture at the indicated pH. The open circles represent the concentration of $VA^{\bullet+}$ when 20 $\mu$M LiP, 2 mM VA, and 200 $\mu$M $H_2O_2$ were mixed together, also in oxygen-saturated reaction mixture at the indicated pH. The closed triangles represent the concentration of $VA^{\bullet+}$ formed by oxidation with Ce(IV) but in an argon-saturated reaction mixture. The open triangles represent the concentration of $VA^{\bullet+}$ formed by oxidation with LiP in an argon-saturated reaction mixture.The concentrations of $VA^{\bullet+}$ were normalized to account for the pH dependence of the rate of oxidation of VA by LiP. The data points are an average of three acquisitions and the error bars represent standard deviations.

steady-state concentration of $VA^{\bullet+}$ [formed by oxidation with Ce(IV) and LiP] at different pH values is shown in Figure 10. The pH-dependent decrease in the steady-state concentration of $VA^{\bullet+}$ in the Ce(IV) oxidation system was found to be due to the decrease in the rate constant for the reaction of Ce(IV) and VA with increasing pH. The steady-state concentration of $VA^{\bullet+}$ normalized at the same rate of $VA^{\bullet+}$ formation was constant in the pH range tested. This served to further confirm that the decay constant is pH-independent. However, the concentration of $VA^{\bullet+}$ in oxygen-saturated solution was lower than its concentration in argon-saturated solution under the same experimental conditions at all pH values. In oxygen-saturated solution the equilibrium for reaction 2 is to the right due to reaction 3, which becomes essentially irreversible. In argon-saturated solution, the decay of $VA^{\bullet}$ is slower and hence protonation proceeded at an appreciable rate, resulting in a higher concentration of $VA^{\bullet+}$, at least under the conditions where the formation rate for $VA^{\bullet+}$ was slow (see Figure 3). Since the p$K_a$ of $VA^{\bullet+}$ has been reported to be $-1.0$ (Khindaria et al., 1995a; Candeias & Harvey, 1995), the equilibrium at the pH values tested predominantly favors the deprotonation of $VA^{\bullet+}$. An increase in pH would favor higher concentrations of $VA^{\bullet}$ and hence its rate of reaction with $O_2$ would increase, depleting $VA^{\bullet+}$. In contrast to the Ce(IV) oxidation system, the steady-state concentration of $VA^{\bullet+}$ formed by oxidation with LiP at various pH values was unaffected by oxygen (Figure 10). This was additional evidence for stabilization of $VA^{\bullet+}$ by LiP. The LiP-bound $VA^{\bullet+}$ must be protected from deprotonation and hence $VA^{\bullet}$ is not available to react with $O_2$.

*Redox Potential of $VA^{\bullet+}$/VA Couple.* Several reports, supporting the role of $VA^{\bullet+}$ as a redox mediator in LiP catalysis, have appeared lately (Chung & Aust, 1995; Goodwin et al., 1995; Koduri & Tien, 1995). Recently, we have demonstrated the reaction of $VA^{\bullet+}$ with oxalate by ESR studies (Khindaria et al., 1995b). The question remains, however, whether the redox potential is sufficient to oxidize lignin. We used cyclic voltammetry to determine the reversible redox potential for $VA^{\bullet+}$/VA couple. In aqueous solution the $VA^{\bullet+}$ was found to be too unstable to allow for the reversible electron transfer. When the sweep rate was increased to overcome this problem, it was realized that the electron transfer between VA and the platinum electrode was not fast enough and the high sweep rates could not be used. The forward peak potential for VA oxidation to $VA^{\bullet+}$ was determined and was 1.28 V vs NHE. The forward peak potential was found to be pH-independent (Figure 11) within experimental error, consistent with the fact that no proton is involved in the oxidation of VA to $VA^{\bullet+}$. The reversible redox potential is always higher by approximately 100−150 mV than the forward peak potential. Hence, even by conservative estimates, it can be predicted that the $VA^{\bullet+}$/VA couple has a redox potential of at least 1.4 V vs NHE, sufficient to oxidize lignin model compounds and lignin. This value was supported by cyclic voltammetry in acetone. The $VA^{\bullet+}$ was more stable in this solvent and the reversible potential for the $VA^{\bullet+}$/VA could be determined at a sweep rate of 20 V/s (Figure 11). The $E^{o}$ in acetone was 1.38 V vs NHE, sufficient to oxidize lignin (Cui & Dolphin, 1990).

## CONCLUDING REMARKS

Lignin and manganese-dependent peroxidases have been implicated in lignin degradation by the white rot fungus *P. chrysosporium* (Kersten et al., 1985; Hammel et al., 1986). This proposal was suspect mainly because of the unlikely direct interaction between the heme and lignin (Poulos et al., 1993). Small molecule "mediators" like $Mn^{2+}$ and VA are thus essential if LiP or the manganese-dependent peroxidases are to oxidize lignin. The "mediators" are oxidized by the peroxidases to $Mn^{3+}$ and $VA^{\bullet+}$, respectively, and in

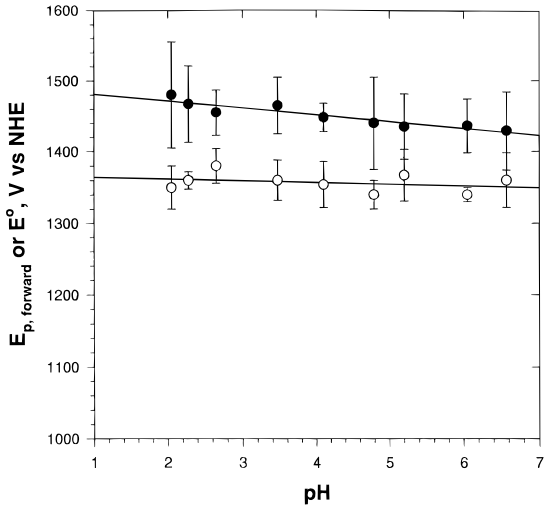


FIGURE 11: Redox potential of the $VA^{\bullet+}$/VA couple as a function of pH. The forward peak potential (●) for the oxidation of VA to $VA^{\bullet+}$ in an aqueous solution and the reversible redox potential (○) for the $VA^{\bullet+}$/VA couple in acetone are plotted as a function of pH. Each datum point is an average of three observations. The data points are an average of three acquisitions and the error bars represent standard deviations.

turn oxidize lignin and or any molecule that cannot approach the heme (Hammel et al., 1994). The "mediators" are themselves reduced back to the parent compounds, $Mn^{2+}$ and VA, respectively. This role of $Mn^{3+}$ has been widely accepted; however, the $VA^{\bullet+}$ was predicted to be too unstable to act as a diffusible oxidant. Indeed, we have also found that $VA^{\bullet+}$ decays at a very rapid rate in bulk solution and would not be expected to act as a diffusible oxidant.

In fact, with a decay constant of $1.2 \times 10^3\ s^{-1}$, the steady-state concentration of $VA^{\bullet+}$ would never exceed 10 nM [$k_{cat}$ of LiP at pH 2.5 (maximum rate), 70 $s^{-1}$, divided by the decay constant], assuming that the LiP concentration in culture is 1 $\mu$M (a high estimate) (Tuisel et al., 1990). Hence, it would not be feasible to propose that $VA^{\bullet+}$ acts as a diffusible oxidant for electron transfer between the heme and lignin.

It was evident, though, from studies where LiP was used to generate $VA^{\bullet+}$, that the $VA^{\bullet+}$ was stabilized by a factor of 700 ($k_{de}$ 1.85 $s^{-1}$). Thus the radical would be stable for a time scale of almost a second and would reach concentrations up to 90% of the LiP concentration in the extracellular medium. It may be argued that if $VA^{\bullet+}$ is stabilized by LiP, it may not be able to interact with lignin, to oxidize it. However, this would be possible if the radical is oriented with the protein in a manner that orbital overlap with external aromatic molecules is possible. According to Marcus' theory of outer-sphere electron transfer, electron transfer can take place up to a distance of 10 Å. Additionally, we have earlier demonstrated that $VA^{\bullet+}$ formed by oxidation with LiP can oxidize both oxalate and malonate (Khindaria et al., 1995b). It is therefore possible for $VA^{\bullet+}$ to act as a redox "mediator" but probably not as a diffusible oxidant. Furthermore, VA is in fact required for lignin depolymerization by the whole cultures of *P. chrysosporium* (Faison & Kirk, 1985).

## REFERENCES

Barr, D. P., & Aust, S. D. (1994) *Environ. Sci. Technol. 28*, 78A−87A.
Barshop, B. A., Wrenn, R. F., & Frieden, C. (1983) *Anal. Biochem. 130*, 134−145.
Buswell, J. A., & Odier, E. (1987) *Crit. Rev. Biotechnol. 6*, 1−60.
Candeias, L. P., & Harvey, P. J. (1995) *J. Biol. Chem. 270*, 16745−16748.
Chance, B. (1952) *Arch. Biochem. Biophys. 41*, 416−424.
Chung, N., & Aust, S. D. (1995) *Arch. Biochem. Biophys. 316*, 733−737.
Cui, F., & Dolphin, D. (1990) *Holzforschung 44*, 279−283.
Dunford, H. B., (1990) in *Peroxidases in Chemistry and Biology* (Everse, J., Everse, K. E., & Grisham, M. B., Eds.) Vol. 2, pp 2−24, CRC Press, Boca Raton, FL.
Faison, B. D., & Kirk, T. K., (1985) *Appl. Environ. Microbiol. 49*, 299−304.
Forney, L. J., Reddy, C. A., Tien, M., & Aust, S. D. (1982) *J. Biol. Chem. 257*, 11455−11462.
Goodwin, D. G., Aust, S. D., & Grover, T. A. (1995) *Biochemistry 34*, 5060−5065.
Hammel, K. E., Kalyanaraman, B., & Kirk, T. K. (1986) *J. Biol. Chem. 261*, 16948−16952.
Hammel, K. E., Mozuch, M. D., Jensen, K. A., Jr., & Kersten, P. J. (1994) *Biochemistry 33*, 13349−13354.
Hammerich, O., & Parker, V. D. (1984) in *Advances in Physical Organic Chemistry* (Gold, V., & Bethell, D., Eds.) pp 55−189, Academic Press, London.
Kersten, P. J., Tien, M., Kalyanaraman, B., & Kirk, T. K. (1985) *J. Biol. Chem. 260*, 2609−2612.
Khindaria, A., Grover, T. A., & Aust, S. D. (1995a) *Biochemistry 34*, 6020−6025.
Khindaria, A., Yamazaki, I., & Aust, S. D. (1995b) *Biochemistry 34*, 16860−16869.
Kirk, T. K., & Farrell, R. L. (1987) *Annu. Rev. Microbiol. 41*, 465−505.
Kuan, I., & Tien, M. (1993) *Proc. Natl. Acad. Sci. U.S.A. 90*, 1242−1246.
Lundquist, K., & Kirk, T. K. (1978) *Phytochemistry 17*, 1676.
Morrisett, J. D. (1976) in *Spin Labelling, Theory and Applications* (Berliner, L. J., Ed.) pp 274−338, Academic Press, New York.
Poulos, T. L., Edwards, S. L., Wariishi, H., & Gold, M. H. (1993) *J. Biol. Chem. 268*, 4429−4440.
Schmidt, K. H., Bromberg, A., & Meisel, D. (1985) *J. Phys. Chem. 89*, 4352−4357.
Tien, M. (1987) *Crit. Rev. Microbiol. 15*, 141−168.
Tien, M., Kirk, T. K., Bull, C., & Fee, J. A. (1986) *J. Biol. Chem. 261*, 1687−1693.
Tuisel, H., Sinclair, R., Bumpus, J. A., Ashbaugh, W., Brock, B. J., & Aust, S. D. (1990) *Arch. Biochem. Biophys. 279*, 158−166.

BI9601666